https://doi.org/10.70882/pahyh878

SCIENCE FORUM (JOURNAL OF PURE AND APPLIED SCIENCES) 26, (5 Special) (2026), 701 - 711

Science Forum (Journal of Pure and Applied Sciences)

Journal Homepage: https://atbuscienceforum.com.ng/index.php/jpas

Semiconductor Materials: Physical and Electrical Properties with Experimental Structural Characterization of Zinc Oxide (ZnO) Using X-Ray Diffraction (XRD)

Mohammed L. Ali[1], Alan Ghafour Tawfeeq[1]. Haval Nooradin Kakaamin[2]

[1]Kirkuk University, College of Education for Pure Sciences

[3]Kirkuk University, College of Sciences

Abstract

Semiconductor materials underpin modern electronic and optoelectronic technologies because their electrical and optical responses can be tailored through composition, structure, and processing. Zinc oxide (ZnO), a widely studied II–VI semiconductor, typically adopts the hexagonal wurtzite crystal structure. This study reviews selected semiconductor fundamentals and reports structural characterization of ZnO powder by X-ray diffraction (XRD). Data were collected with a PANalytical diffractometer using Cu Ka radiation (λ = 0.15406 nm) at 45 kV and 40 mA. The scan covered 2θ = 20°–60° with a step size of 0.015°. Five diffraction reflections were reported at 32.443°, 34.778°, 36.940°, 48.295°, and 57.875°, and indexed to the (100), (002), (101), (102), and (110) planes, respectively. Their positions are consistent with the hexagonal wurtzite phase of ZnO. The crystallite size was reported as 34.4 nm, estimated from the (002) reflection using the Debye–Scherrer method. However, the numerical full width at half maximum (FWHM) and any correction for instrumental broadening were not provided. Consequently, the reported size cannot be independently reproduced or verified from the available information and should be interpreted as an estimate. The presented measurements establish the phase-consistent diffraction features of the powder within the stated angular range; they do not, by themselves, determine optical or electrical performance. The experimental scope is therefore limited to structural characterization. Further work should report peak-width data and the procedure for instrumental-broadening correction to support crystallite-size analysis. Complementary optical and electrical measurements are also needed to assess the material's functional properties and its potential suitability for device applications.

Keywords

Debye-Scherrer Equation, Semiconductor Materials, Zinc oxide (ZnO), X-ray Diffraction (XRD), Wurtzite Structure, Crystallite Size.

EISSN: 3156-5190 (Online)
ISSN: 1119-4618 (Print)
JPAS
Faculty of Science, ATBU Bauchi

Corresponding Author: Mohammed L. Ali, Kirkuk University, College of Education for Pure Sciences. Email: mohammedlateef@uokirkuk.edu.iq[1]
alan.00742510@gmail.com[2] haval.00210142@gmail.com[3]

© 2026 Faculty of Science, ATBU Bauchi. All rights reserved

1. INTRODUCTION

Materials science examines the relationships among a material's structure, properties, processing, and performance. Understanding these relationships helps researchers select and develop materials for technological applications [1]. Semiconductors are especially important because their electrical conductivity can be controlled by temperature, doping, and illumination. They are therefore essential components of modern electronic and optoelectronic devices, including diodes, transistors, solar cells, and sensors [2].

Previous studies have investigated the structural characteristics of zinc oxide (ZnO) using X-ray diffraction (XRD) and complementary techniques. Kaygili et al. examined synthesized ZnO powder through experimental and theoretical approaches, including XRD, FTIR, SEM, and EDX [3]. Djouadi et al. synthesized ZnO nanopowder by a hydrothermal route and reported its hexagonal wurtzite structure [4]. Al-Weally et al. investigated the structural, optical, and morphological properties of ZnO nanoparticles and nanorods using XRD, UV–Visible spectroscopy, and FE-SEM [5]. These studies demonstrate the value of structural characterization. The present work reviews selected semiconductor fundamentals and focuses experimentally on the XRD characterization of ZnO powder.

The XRD results reported for the investigated ZnO powder show reflections assigned to the (100), (002), (101), (102), and (110) planes. These reflections are consistent with the hexagonal wurtzite structure; the measured peak positions are discussed in Section 4.

2. FUNDAMENTALS OF SEMICONDUCTOR MATERIALS

2.1 Definition and Classification

Semiconductors have electrical conductivity between that of conductors and insulators. Unlike metals, their conductivity can vary with temperature, illumination, and the introduction of controlled impurities. This controllability makes them important in electronic and optoelectronic applications [6], [7].

Based on composition, semiconductors are classified as elemental or compound materials. Elemental semiconductors contain one type of atom, such as silicon (Si) and germanium (Ge), whereas compound semiconductors contain two or more elements, such as zinc oxide (ZnO) and gallium arsenide (GaAs). They may also be classified as intrinsic or extrinsic according to the origin and concentration of charge carriers [6], [8].

An intrinsic semiconductor is ideally pure, and its charge carriers are generated mainly by thermal excitation; electron and hole concentrations are equal. In an extrinsic semiconductor, controlled impurity atoms (dopants) modify the carrier concentration. This process is known as doping [6], [8].

Extrinsic semiconductors are classified as n-type or p-type. Donor impurities provide additional electrons, making electrons the majority carriers in n-type materials. Acceptor impurities create additional holes, making holes the majority carriers in p-type materials [6], [7].

2.2 Physical and Electrical Properties

Semiconductor behavior depends on crystal structure, chemical composition, energy band gap, carrier concentration, and carrier mobility. Defects and impurities can also affect electrical and optical responses. Therefore, structural and electronic properties should be considered together when evaluating a semiconductor [6], [7].

Electrons in the conduction band and holes in the valence band are the principal charge carriers in semiconductors. Their concentrations and mobilities determine electrical conductivity, as expressed in Equation (1), where q is the elementary charge, n and p are electron and hole concentrations, and μ_n and μ_p are their respective mobilities [1], [2], [9].

$$\sigma = q(n\mu_n + p\mu_p) \quad (1)$$

Equation (1) describes the combined contributions of electrons and holes to semiconductor conductivity. Both carrier concentration and mobility influence the resulting conductivity [6], [8].

Temperature can excite electrons from the valence band to the conduction band, generating electron–hole pairs. The resulting carrier concentration and conductivity also depend on doping and material defects [6], [8].

$$V = IR \quad (2)$$

Ohm's law (Equation (2)) relates voltage (V), current (I), and resistance (R) for an ohmic sample. Although semiconductor devices may exhibit nonlinear current–voltage behavior under some operating conditions, this relation applies to ohmic behavior. Semiconductors also interact with light through photon absorption and emission. Absorption can generate an electron–hole pair when the photon energy is sufficient to cross the band gap [6], [8].

2.3 Energy Band Theory

Energy-band theory explains the electrical behavior of solids by describing the allowed electron-energy ranges. The valence band is normally occupied at low temperatures, whereas electrons in the higher-energy conduction band can contribute to electrical conduction [6], [7].

The forbidden energy gap, or band gap (E_g), is the energy interval between the valence-band maximum and conduction-band minimum in which no allowed electronic states exist in an ideal crystal. Thermal energy or absorbed light can excite electrons across this gap, leaving holes in the valence band [6], [8].

$$E_g = E_c - E_v \quad (3)$$

Equation (3) defines the band-gap energy as the difference between the conduction-band minimum and valence-band maximum. In a direct-band-gap

semiconductor, these extrema occur at the same crystal momentum, allowing optical transitions without phonon assistance. In an indirect-band-gap material, the extrema occur at different momenta and a phonon is generally required to conserve momentum. This distinction is important when discussing semiconductor optical behavior [1], [2], [6],[9].

$$E_{ph} = h\nu = \frac{hc}{\lambda} \quad (4)$$

Equation (4) relates photon energy to frequency and wavelength, where h is Planck's constant, v is frequency, c is the speed of light, and λ is wavelength. A photon must have sufficient energy to promote a band-to-band transition [1], [2], [9].

$$n_i = \sqrt{N_c N_v}\, exp\left[-\frac{E_g}{2k_B T}\right] \quad (5)$$

Equation (5) describes intrinsic carrier concentration at thermal equilibrium. Here, k_B is Boltzmann's constant, T is absolute temperature, and N_c and N_v are the effective densities of states in the conduction and valence bands, respectively [6],[8].

2.4. Structural Characterization of Semiconductor Materials

The physical and electrical characteristics of semiconductors are strongly influenced by their crystal structures. X-ray diffraction (XRD) is a non-destructive technique used to identify crystalline phases, examine lattice structures, and assess crystallinity through diffraction from atomic planes [10].

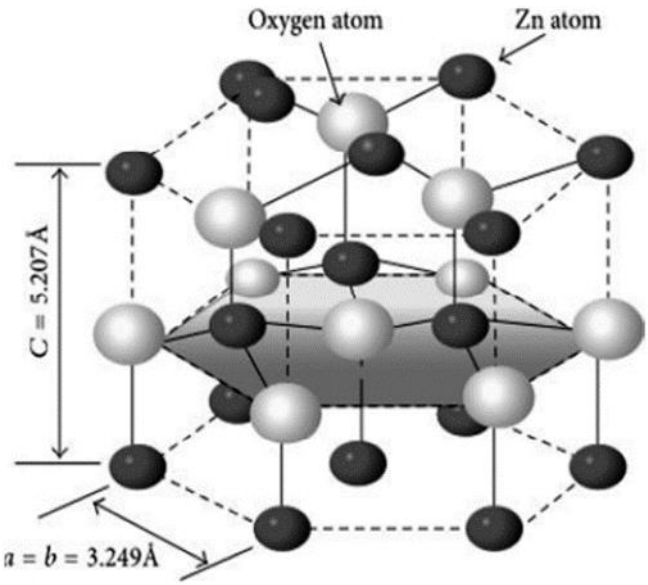


Figure 1: ZnO's Crystalline Structure

X-ray diffraction (XRD) analysis is a valuable technique for confirming the hexagonal crystal structure of zinc oxide (ZnO) and identifying the characteristic diffraction planes associated with its wurtzite structure [11].

3. ZINC OXIDE (ZnO)

3.1. General Introduction to ZnO

Zinc oxide (ZnO) is an inorganic II–VI compound semiconductor with a stable hexagonal wurtzite structure under ambient conditions. It has a direct band-gap energy of approximately 3.37 eV and an exciton binding energy of about 60 meV, properties that have motivated extensive research into UV-related and optoelectronic applications [12].

ZnO can be prepared as bulk crystals, thin films, nanoparticles, nanorods, and nanowires. Its properties depend on preparation conditions, morphology, crystal quality, dimensions, defects, and composition; therefore, the characteristics of each sample should be evaluated individually [12], [13].

3.2. Crystal Structure of ZnO

At ambient conditions, ZnO most commonly crystallizes in the hexagonal wurtzite structure. It consists of interpenetrating Zn and O sublattices, with each ion tetrahedrally coordinated by four ions of the opposite type. This arrangement produces hexagonal symmetry and a polar axis along the crystallographic c-direction [12].

The absence of a center of symmetry in wurtzite ZnO is associated with polar and piezoelectric behavior. Wurtzite is the stable ambient structure, although other structures may occur under particular growth conditions or pressure [12].

XRD is commonly used to investigate ZnO crystallinity. Measured peak positions can be compared with reference diffraction data to identify phases and assign crystallographic planes. They can also be used to determine interplanar spacing and lattice parameters. Peak broadening may provide an estimate of coherent crystallite-domain size when instrumental broadening is considered. XRD alone does not measure electrical conductivity or optical band gap.

3.3. Physical and Chemical Properties

ZnO is a chemically stable metal-oxide semiconductor. Its physical behavior can be influenced by grain boundaries, particle size, porosity, crystal quality, defects, and impurities. Surface chemistry can be particularly important in nanostructured ZnO because of its high surface-to-volume ratio [12], [13].

The polar, non-centrosymmetric wurtzite structure is associated with spontaneous polarization and piezoelectricity. These properties are relevant to sensors and piezoelectric energy-harvesting devices [13].

ZnO nanostructures can be produced by hydrothermal, sol–gel, chemical precipitation, electrochemical deposition, and vapor-based methods. Different preparation routes can lead to variations in particle size, morphology, surface states, and defect density [12], [13].

3.4. Electrical and Optical Properties

ZnO is widely reported as a direct wide-band-gap semiconductor, with a band gap of approximately 3.37 eV at room temperature. Its optical response may include near-band-edge ultraviolet emission and defect-related visible emission; the observed

spectra depend on sample quality and measurement conditions [12].

The electrical conductivity of ZnO depends on carrier concentration and mobility. Undoped ZnO is often reported to exhibit n-type conductivity, but the origin and stability of this behavior may depend on growth conditions, post-growth treatment, defects, and unintentional impurities [12].

Doping and control of defects or microstructure can modify ZnO's electrical and optical properties, which are relevant to sensors, light-emitting devices, UV photodetectors, and transparent conducting layers. These are literature-reported properties and were not measured by XRD in the present work [12], [13].

ZnO is widely reported to have a direct band gap of approximately 3.37 eV at room temperature. This is a literature value, not an experimental result of the present study, which was limited to XRD. UV–Vis absorption spectroscopy would be required to estimate the band gap of the examined sample [14].

3.5. Applications of ZnO

Reported applications of ZnO include UV photodetectors, optoelectronic devices, gas and chemical sensors, photocatalysis, and piezoelectric energy harvesting [12], [13].

Nanorods, nanowires, nanoparticles, and hierarchical ZnO structures are investigated because synthesis conditions can tailor morphology and surface properties. Their performance depends on dimensions, defects, surface chemistry, and device design [12], [13].

4.Experimental Work and XRD Analysis

4.1 Introduction

This section presents the XRD procedure and structural findings for the ZnO powder. XRD produces characteristic diffraction peaks when monochromatic X-rays interact with periodically arranged atomic planes. The recorded pattern is compared with reference powder-diffraction data to identify crystalline phases [15], [16].

4.2 Principle of X-Ray Diffraction

XRD is based on constructive interference of X-rays scattered by parallel atomic planes. The condition for diffraction is expressed by Bragg's law:

$$n\lambda = 2d\ sin\ \theta$$

Here, d is the interplanar spacing, θ is the Bragg angle, n is the diffraction order, and λ is the X-ray wavelength. Because the diffractometer records 2θ, the Bragg angle is half the reported value. Peak positions can then be compared with reference data to identify phases and crystallographic planes [16], [17].

4.3 XRD Instrumentation and Experimental Conditions

The structural measurements were performed using a PANalytical diffractometer with a Cu X-ray tube (λ = 0.15406 nm). The reported setup included a nickel filter to absorb Cu Kβ radiation, a 1 × 1 mm^2 point focus, a 1 mm-diameter collimator, and a four-circle goniometer [16].



Figure 2. PANalytical X-ray diffractometer.

Table 1. Experimental parameters and operating conditions of the X-ray diffractometer used for ZnO sample characterization.

Experimental parameter	Condition reported in the manuscript
Diffractometer	PANalytical
X-ray source	Cu X-ray tube
Wavelength, λ	0.15406 nm
Tube voltage	45 kV
Tube current	40 mA
Scanning mode	2θ/θ scanning mode
2θ scanning range	20°–60°
Step size	0.015°
Beam focus	1 × 1 mm^2 point focus
Filter	Nickel filter to absorb Cu Kβ radiation
Collimator	1 mm diameter
Sample mounting	Four-circle goniometer

4.4 XRD Data Collection

The ZnO powder was measured in 2θ/θ scanning mode over 20°–60°, using a step size of 0.015°. The Cu X-ray tube operated at 45 kV and 40 mA. Peak positions were identified from the diffraction pattern and compared with conventional powder-diffraction data [17]. The available experimental description does not specify sample mass or preparation, scan speed or counting time, background correction, or peak-fitting parameters; these details are therefore not assumed in this paper.

4.5 XRD Results and Peak Assignment

Five principal diffraction peaks are reported at 2θ = 32.443°, 34.778°, 36.940°, 48.295°, and 57.875°, assigned respectively to the ZnO planes (100), (002), (101), (102), and (110) [17]. The reported peak positions and plane assignments are summarized in Table 2.

Table 2. XRD peak positions (2θ) and corresponding crystallographic planes (hkl) of the ZnO sample.

Peak	2θ (degree)	Assigned plane (hkl)
1	32.443	(100)
2	34.778	(002)
3	36.940	(101)
4	48.295	(102)
5	57.875	(110)

The five peak positions and assignments are reproduced from the source manuscript. The original XRD pattern is retained; no new diffraction curve or intensity data have been generated because the numerical intensity-versus-2θ dataset was not available.

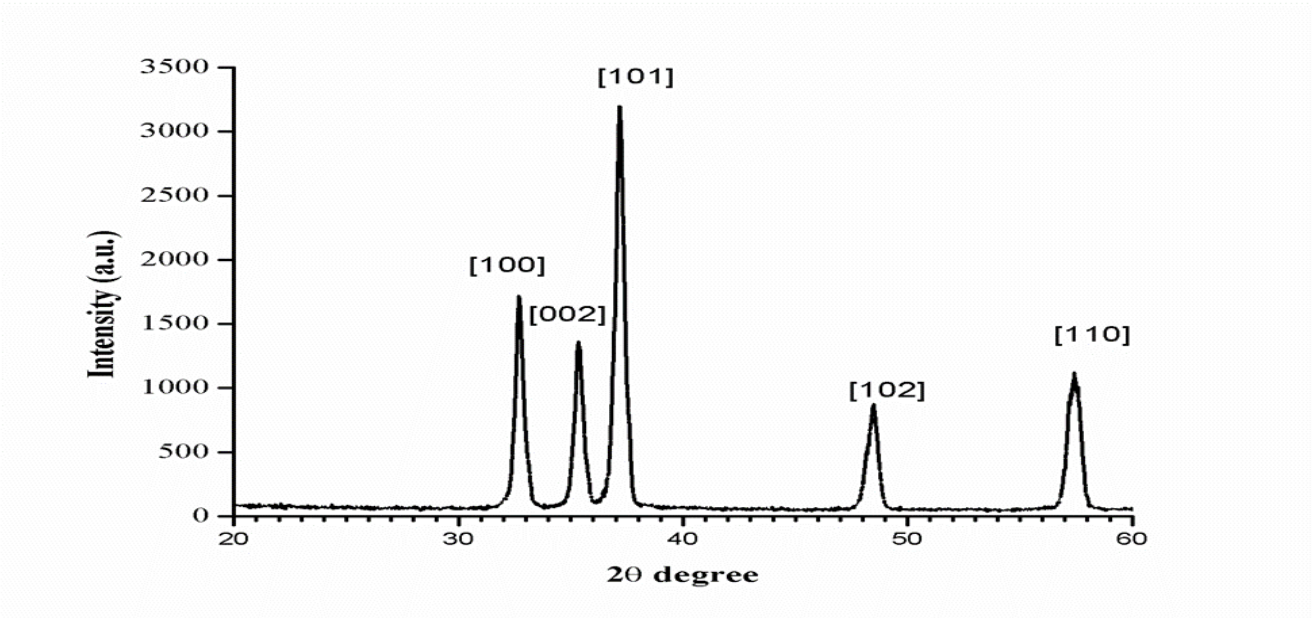


Figure 3. XRD diffraction pattern of ZnO powder

4.6 Crystallite Size Estimation

According to the original publication, the Debye-Scherrer technique was used to determine the average crystallite size based on the line width of the (002) diffraction peak. The formula is:

$$D = \frac{K\lambda}{\beta \cos\theta}$$

In this equation, D is the mean coherent crystallite-domain size, K is the shape factor, λ is the X-ray wavelength, β is the full width at half maximum (FWHM) in radians, and θ is the Bragg angle of the selected reflection [15].

The source manuscript reports a crystallite size of 34.4 nm from the (002) reflection. However, the numerical FWHM, shape factor, and instrumental-broadening correction are not provided. Consequently, the value cannot be independently reproduced from the available information and is retained only as a reported result.

4.7 Discussion of the Structural Results

Within the measured range of 20°–60°, five reflections were assigned to ZnO: (100), (002), (101), (102), and (110). The source manuscript reports a

crystallite-domain size of approximately 34.4 nm from the (002) reflection using the Scherrer method [17]. These assignments should be checked against the complete original pattern and a verified reference card before making a definitive phase-purity claim.

The XRD measurements provide structural information only. Electrical conductivity, carrier concentration, and optical band-gap energy cannot be inferred from the diffraction pattern alone because they require separate electrical and optical measurements.

5. Conclusions

This study reviewed selected semiconductor fundamentals and used X-ray diffraction (XRD) to examine the structure of ZnO powder. The experimental investigation was limited to the crystalline structure of the sample.

Measurements were reported using a PANalytical diffractometer with Cu radiation (λ = 0.15406 nm), at 45 kV and 40 mA. The diffraction pattern was recorded over 2θ = 20°–60° with a step size of 0.015°.

Five diffraction peaks were reported at 2θ = 32.443°, 34.778°, 36.940°, 48.295°, and 57.875°, assigned to the (100), (002), (101), (102), and (110) planes, respectively.

The reported peak positions and indexing are consistent with the hexagonal wurtzite structure commonly associated with ZnO. However, confirmation of phase purity requires evaluation of the complete diffraction pattern against an appropriate reference database.

A crystallite size of approximately 34.4 nm was reported from the (002) reflection. This value represents a coherent diffraction-domain estimate, not necessarily the physical particle size. It cannot be independently verified without the numerical FWHM and instrumental-broadening information.

Overall, the XRD results support structural characterization of the ZnO powder but do not determine its band gap, carrier concentration, or electrical conductivity. UV–Vis spectroscopy, microscopy, and electrical measurements would be required to investigate these additional properties.

5.1. Recommendations for Future Work

For reproducible diffraction analysis and crystallite-size estimation, report the complete intensity dataset, peak intensities, and FWHM values.

Apply instrumental-broadening correction before using peak widths for crystallite-size estimation; complementary line-profile methods may also be considered.

Use complementary techniques, such as UV–Vis spectroscopy for optical absorption and SEM for morphology, when these properties are within the study scope.

Conduct suitable electrical measurements to determine conductivity, resistivity, and charge-carrier characteristics.

REFERENCES

[1] "Materials Science and Engineering: An Introduction, 10th Edition | Wiley," Wiley.com. Accessed: Nov. 02, 2026. [Online]. Available: https://www.wiley.com/en-us/materials-science-and-engineering-an-introduction-10th-edition-p-9781119405498

[2] D. A. Neamen, *Semiconductor Physics and Devices: Basic Principles*. McGraw-Hill, 2012.

[3] O. Kaygili *et al.*, "An experimental and theoretical investigation of the structure of synthesized ZnO powder," *Chem. Phys.*, vol. 513, pp. 273–279, Sep. 2018, doi: 10.1016/j.chemphys.2018.08.021.

[4] "Structural and morphological characterizations of ZnO nanopowder synthesized by hydrothermal route using inorganic reactants - IOPscience." Accessed: Nov. 06, 2026. [Online]. Available: https://iopscience.iop.org/article/10.1088/1674-4926/35/12/123001

[5] D. Hadi Al-Weally, A. Mebdir Holi, and A. Abdullah AL-Zahrani, "Structural, Optical, Morphological Properties of ZnO Nanoparticle/ZnO Nanorods," *J. Phys. Conf. Ser.*, vol. 1294, no. 2, p. 022030, Sep. 2019, doi: 10.1088/1742-6596/1294/2/022030.

[6] "Solid State Physics," TU Delft OCW. Accessed: Nov. 02, 2026. [Online]. Available: https://ocw.tudelft.nl/courses/solid-state-physics/

[7] "Semiconductor Physics - theory and experiments. A short introductory undergraduate course. | Zenodo." Accessed: Nov. 02, 2026. [Online]. Available: https://zenodo.org/records/7560889

[8] "Semiconductor Devices: Theory and Application," Open Textbook Library. Accessed: Nov. 02, 2026. [Online]. Available: https://open.umn.edu/opentextbooks/textbooks/semiconductor-devices-theory-and-application?utm_source=chatgpt.com

[9] Ü. Özgür *et al.*, "A comprehensive review of ZnO materials and devices," *J. Appl. Phys.*, vol. 98, no. 4, p. 041301, Aug. 2005, doi: 10.1063/1.1992666.

[10] X. Zhao, R. Liao, N. Liang, L. Yang, J. Li, and J. Li, "Role of defects in determining the electrical properties of ZnO ceramics," *J. Appl. Phys.*, vol. 116, no. 1, 2014, Accessed: Nov. 02, 2026. [Online]. Available: https://pubs.aip.org/aip/jap/article/116/1/014103/139110

[11] V. Parihar, M. Raja, and R. Paulose, "A Brief Review of Structural, Electrical and Electrochemical Properties of Zinc Oxide Nanoparticles," *Rev. Adv. Mater. Sci.*, vol. 53, no. 2, pp. 119–130, Feb. 2018, doi: 10.1515/rams-2018-0009.

[12] S. Baskoutas, Ed., *Zinc Oxide Nanostructures: Synthesis and Characterization*. MDPI - Multidisciplinary Digital Publishing Institute, 2018. doi: 10.3390/books978-3-03897-303-4.

[13] B. E. Zein, Ed., *Novel ZnO-Based Nanostructures*. MDPI - Multidisciplinary Digital Publishing Institute, 2023. doi: 10.3390/books978-3-0365-7135-5.

[14] M. A. Borysiewicz, "ZnO as a Functional Material, a Review," *Crystals*, vol. 9, no. 10, p. 505, Oct. 2019, doi: 10.3390/cryst9100505.

[15] Y. T. Prabhu, K. V. Rao, V. S. S. Kumar, and B. S. Kumari, "X-Ray Analysis by Williamson-Hall and Size-Strain Plot Methods of ZnO Nanoparticles with Fuel Variation," *World J. Nano Sci. Eng.*, vol. 4, no. 1, pp. 21–28, Mar. 2014, doi: 10.4236/wjnse.2014.41004.

[16] "Synthesis, Properties, and Applications of Oxide Nanomaterials | Wiley Online Books." Accessed: Nov. 02, 2026. [Online]. Available: https://onlinelibrary.wiley.com/doi/book/10.1002/0470108975

[17] E. H. Kisi and M. M. Elcombe, "u parameters for the wurtzite structure of ZnS and ZnO using powder neutron diffraction," *Acta Crystallogr. C*, vol. 45, no. 12, pp. 1867–1870, Dec. 1989, doi: 10.1107/S0108270189004269.